

Cotranslational folding of deeply knotted proteins

Mateusz Chwastyk and Marek Cieplak

Institute of Physics, Polish Academy of Sciences, Al. Lotników 32/46, 02-668 Warsaw, Poland

September 12, 2021

Abstract

Proper folding of deeply knotted proteins has a very low success rate even in structure-based models which favor formation of the native contacts but have no topological bias. By employing a structure-based model, we demonstrate that cotranslational folding on a model ribosome may enhance the odds to form trefoil knots for protein YibK without any need to introduce any non-native contacts. The ribosome is represented by a repulsive wall that keeps elongating the protein. On-ribosome folding proceeds through a slipknot conformation. We elucidate the mechanics and energetics of its formation. We show that the knotting probability in on-ribosome folding is a function of temperature and that there is an optimal temperature for the process. Our model often leads to the establishment of the native contacts without formation of the knot.

1 Introduction

There are several hundreds of knot-containing structures [1, 2, 3] in the Protein Data Bank (PDB) and their topology can be characterized primarily by how many intersections a backbone makes with itself on making its two-dimensional projection. The knot extends between two end points, n_1 and $n_2 > n_1$, along the sequence. The knot ends are defined operationally through systematic cutting-away of the amino acids from both termini until the knot disintegrates [4, 5]. The last site that still supports the knot is its end point. If n_1 and n_2 are both distant from the termini, the knot is considered to be deep; otherwise it is called shallow. One needs closed lines to declare existence of a knot on a line with certainty. Backbones of proteins are generally not closed but for deep knots the determination of a knot-type is quite reliable.

Stretching of a knotted protein either at constant speed [6, 7, 8] or at constant force [9] results in a step-wise knot tightening process in which the knot ends jump. Here, we consider two other conformation changing processes [10] in knotted proteins: folding and unfolding through heating. Folding from an extended state to a knotted native conformation of protein YibK has been reported [11, 12] to be difficult with, at best, 1 - 2% success rate even if one uses a coarse-grained structure-based model. Here, we examine whether nascent conditions, such that exist when a protein is formed by the ribosome [13, 14, 15, 16], can help in establishing the native knot in proteins. We propose a simple generic model in which the ribosome is represented as an infinite repulsive plate which spawns proteins. Our model is an oversimplification of the real geometry of the ribosome – the peptide chain is formed in the ribosome tunnel and it undergoes folding, at least partially, within it. The tunnel has a diameter that varies between 10 and 20 Å and the largest cavity in the tunnel cannot encompass a sphere with a radius larger than 9.5 Å [13, 17, 18]. This geometry provides stronger confinement than that induced by the plane. Nevertheless, the model with the plane is the simplest one that introduces new qualitative features that are brought in by confinement.

Here, our focus is on YibK [20] from *Haemophilus influenzae* which contains a deep trefoil knot with three intersections. The corresponding PDB code is 1J85. (We shall refer to proteins through their PDB structure codes.) This protein is probably the most frequently cited example of a deeply knotted protein [1, 2]. Its radius of gyration is about 15 Å. We find that the nascent conditions do help in folding 1J85 – they actually enable it – and the effect is observed only within a range of temperatures that provide optimality. We show that invoking non-native contacts is not necessary to generate the on-ribosome slipknot, just one needs to employ a proper procedure to define contacts that are declared native. We identify the slipknot based mechanism of folding and explain why the model ribosome favors its formation. We also study the energetics involved in the emergence of the slipknot. Unlike the claims of ref. [11] (that uses the same model), we do not observe the slipknot in the absence of the ribosome.

2 Structure-based modeling

The justification and details of implementation of our model are explained in refs. [22, 23, 24]. Its character is structure-based or, equivalently, Go-like [21], and the molecular dynamics deals only with the α -C atoms. The bonded interactions are described by the harmonic potentials. The list of pairs of amino acids that are considered to be in contact (*i.e.* interacting) in the native state is known as the contact map. These contacts are described by the Lennard-Jones potentials with the minima at the crystallographically determined distances. The potentials are identical in depth, denoted as ϵ . The value of ϵ has been calibrated by making comparisons to the experimental data on stretching: approximately, $\epsilon/\text{\AA}$ is 110 pN (which also is close to the energy of the O-H-N hydrogen bond of 1.65 kcal/mol). Non-native contacts are considered repulsive.

The contact map itself is obtained by using the overlap criterion in which the heavy atoms in the native conformation are represented by enlarged van der Waals spheres [22, 25]: if at least one pair of such spheres placed on different amino acids overlap (OV) then there is the native contact. An alternative way to establish a contact map is by invoking considerations that are more chemical in nature, as available at the CSU server [26]. The CSU contacts may either be specific (like hydrogen bonds) or non-specific (presumably the much weaker dispersive interactions). The CSU and OV maps have many contacts in common but are not identical. Thus, in addition to the OV map, we also consider OV-CSU map in which we augment CSU by the missing specific CSU contacts.

The backbone stiffness is accounted for by the chirality potential [22]. The simulations are done at various temperatures. For most proteins without any knots, optimal folding takes place around at $T = 0.3 \epsilon/k_B$, which should correspond to a vicinity of the room temperature (k_B is the Boltzmann constant). We generate at least 200 trajectories for each temperature considered. The time unit of the simulations, τ , is effectively of order 1 ns as the motion of the atoms is dominated by diffusion instead of being ballistic.

Folding is usually declared when all native contacts are established for the first time. For knotted proteins, however, this condition does not necessarily signify that the correct native knot has been formed.

There are two important aspect of the role of the ribosome in the context of nascent folding. The first is that folding of a protein is concurrent with its birth. Since the mRNA is translated from 5' to 3', the proteins are synthesized from the N terminus to the C terminus. The time interval between the emergence of two successive α -C atoms will be denoted by t_w . The second aspect is that the surface of the ribosome provides excluded volume and, therefore, reduces the conformational entropy. Both aspects can be captured by a model in which the ribosome is represented by an infinite plate which gives birth to a protein at one fixed location. We take the plate to generate a laterally uniform potential of the form $\frac{3\sqrt{3}}{2} \epsilon (\frac{\sigma_0}{z})^9$, where z denotes the distance away from the

plate and $\sigma_0 = 4 \times 2^{-1/6} \text{ \AA}$. This form of the potential comes from integrating the energy of interaction between a Lennard-Jones particle and a semi-infinite continuum below $z=0$ and discarding the attractive part. A coarse-grained model of cotranslational folding with molecularly sculpted ribosome has been proposed by Elcock [27]. We have adopted a less sophisticated model in order to enable simulations of hundreds of trajectories that last long – formation of a deep knot is a rare event – and making simplifications is necessary.

3 Results

The PDB structure file of 1J85 provides coordinates of 156 residues. About half of them are arranged into seven α -helices and eight β -strands [20]. The native conformation of 1J85 is shown in panel A of Fig. 1. Segments 1-74, 75-95, 96-120, and 121-156 are shown in green, red, green, and purple respectively. The reason for this color convention is that in order to form the knot in (at least) cotranslational folding, the purple segment (121-141) must form a slip-loop that would go through the red knot-loop (see the defining drawings in ref. [28]). The knot ends are at LEU-75 and LYS-119 in the native state – a separation of 44 sites. On stretching, the knot tightens up and the ultimate separation between the knot ends becomes 10 [6, 9].

3.1 Equilibrium properties and thermal unfolding

In order to set the stage, we first consider a situation in which 1J85 is set in the native state and then undergoes time evolution at various temperatures. At any finite T , some number of contacts break down (the distance between the α -C atoms in residues that make a contact becomes larger than 1.5 of the native distance) and some get restored. The top panel of Fig. 2 shows the probability, P_0 , of all native contacts being *simultaneously* established as a function of T . Similar to the lattice models of proteins [29] (see also an exact analysis [30, 31]) one may define T_f as a temperature at which P_0 crosses through $\frac{1}{2}$. For the OV contact map, $T_f = 0.194 \text{ } \epsilon/k_B$ and for the OV-CSU contact map it is $0.204 \text{ } \epsilon/k_B$ – just a small shift. For both of these contact maps, P_0 is essentially close to zero at $T = 0.3 \text{ } \epsilon/k_B$ (1% and 3% for OV and OV-CSU respectively). However, at this temperature, the fraction of the native contacts present, Q , is high (the middle panel of Fig. 2). Q crosses $\frac{1}{2}$ at 0.827 and $0.908 \text{ } \epsilon/k_B$ for OV and CSU-OV respectively. Folding is said to occur when all native contacts are established simultaneously and the kinetic optimality (typically around $0.3 - 0.35 \text{ } \epsilon/k_B$) may take place where P_0 is small.

It should be noted that in ref. [11] T_f is defined as corresponding to the temperature at which a half of the native bonds are present (*i.e.* around $0.8 \text{ } \epsilon/k_B$) – a much more relaxed criterion compared to P_0 crossing $\frac{1}{2}$. At this elevated temperature, substantially higher than the room temperature, the probability of maintaining the native conformation is simply zero. However, the temperature at which Q crosses $\frac{1}{2}$ signals the onset of globular shapes in the model protein. The simulations reported on in ref. [11] could have been done around the T_f defined through $Q = \frac{1}{2}$ as this is the only temperature mentioned in the text.

The fluctuations in the contact occupation numbers may or may not affect the sequential locations of the knot ends. Fig. 3 shows locations of the knot in examples of trajectories at several temperatures. At $T = 0.3 \text{ } \epsilon/k_B$, the knot ends stay fixed for at least $20\,000\,000 \text{ } \tau$ – a duration which is at least three orders of magnitude longer than optimal folding times of unknotted proteins within the same model [32]. At $T = 1.00 \text{ } \epsilon/k_B$, the knot ends stay put for a while and then diffuse out of the chain rapidly. At $t = 0.95 \text{ } \epsilon/k_B$ we observe an intermittent behavior in which the knot disappears and is then restored. If there is any intermittency at $T = 0.9 \text{ } \epsilon/k_B$, then the recovery time is longer than the scale of the simulations. The bottom panel of Fig. 2 shows the median unfolding time defined as in ref. [33], *i.e.* through the instant at which all contact that are sequentially

separated by more than l are broken simultaneously. Taking l of 4 (local helical contacts) was numerically unfeasible so we took $l = 10$. The statistics were based on 110 trajectories. At $T = 1.0 \epsilon/k_B$ and below less than 50% trajectories led to folding and the median time could not be determined – with the cutoff of 30 000 τ .

3.2 Folding in unbounded space

We now consider folding in an unbounded space when one starts from a random conformation which is nearly fully extended. Even though we use the same model as in ref. [11], we do not find even one single trajectory that would lead to correct folding. However, there were trajectories which led to the establishment of all native contacts in an unknotted way. We shall refer to such situations as corresponding to misfolding. One of them is shown in panel C of Fig. 1. The lack of proper folding in 1J85 essentially agrees with the result of ref. [12] (where 0.1% success rate is reported). We have generated 1201 trajectories at $0.35 \epsilon/k_B$ and between 200 and 314 trajectories at 0.1, 0.2 and $0.3 \epsilon/k_B$. The simulational cutoff time was 1 000 000 τ . With this statistics, a 1 - 2% success rate claimed in ref. [11] (at unspecified temperatures) would mean observation of good folding in at least 12 trajectories. We speculate that the discrepancy may be due to the following factors a) possible biases in the initial conformations used in that reference, b) malfunctioning of the KMT algorithm (that may show knots when none are present), and c) the folding temperature range is narrower than $0.025 \epsilon/k_B$, i.e. the steps we considered, and the right T to fold was found accidentally. It should be noted that we have obtained a total of 338 misfolded trajectories (17% of all trajectories). 143 of these are at $0.35 \epsilon/k_B$ and correspond to a mean folding time of 472 651 τ . It is possible to mistake some of the misfolded states for the knotted ones. We find no folding nor misfolding at T_f defined by the condition of $Q = \frac{1}{2}$.

Not much is changed when one attempts to reduce the conformational entropy by anchoring the C terminus. For the total of 427 trajectories (with T between 0.1 and $0.4 \epsilon/k_B$) 93 (i.e. 22%) established all native contacts without forming the knot.

We have also considered a different Go-like model, along the lines of Clementi *et al.* [34]. In this model, the backbone stiffness is accounted for by the more common bond and dihedral angle potentials. The contact interactions are given by the 10-12 Lennard-Jones potentials, and we take the contact map to be given by OV (here we removed the $i, i+2$ and $i, i+3$ contacts). For this model, T_f moves upward by about $0.2 \epsilon/k_B$ and P_0 is about 0.01 at $0.6 \epsilon/k_B$. At this T , only one out of 246 trajectories led to the correct folding with the proper knot (the folding time was 510 264 τ). At temperatures $0.7 \epsilon/k_B$ and $0.75 \epsilon/k_B$ we get 1% and 7% of the correctly folded trajectories respectively and none at lower temperatures. This model, however, is not the one considered in ref. [11].

3.3 Folding on the ribosome

The percentage-wise success, S , of reaching the properly knotted folded conformation increases substantially by simulating the process in the cotranslational way. The results are summarized in Fig. 4. They depend on the value of t_w but there appears to be a saturation in S around t_w of 5 000 τ . The experimental times of translation are certainly much longer than $\sim 5 \mu s$ but this is not expected to affect the S . However, the corresponding S for misfolding (the inset in the lower panel) may reach saturation at a bigger t_w .

The data for the evidently optimal $0.35\epsilon/k_B$ were obtained based on 500 trajectories for each t_w that was considered. Same statistics were used for 0.325 and $0.375 \epsilon/k_B$ and t_w of 5 000 τ . In other cases, there were at least 100 trajectories. The average combined time of folding under the optimal conditions with $t_w = 5000 \tau$ is 860353 τ . Comparable times are at 0.325 and $0.375 \epsilon/k_B$.

Interestingly, switching to the Clementi *et al.*-like model generates no proper folding independent of whether the contact map is OV, CSU, or OV-CSU (in the temperature

range between 0.45 and 1.3 ϵ/k_B). The backbone chain appears to be too stiff to allow for a knot in this model.

The lower panel of Fig. 4 shows that the time evolution from extended states results in a substantial percentage of the misfolded conformations. This percentage gets boosted by the nascent conditions from 33% to 37% if the evolution takes place at $0.3\epsilon/k_B$. At this T , there is no knotted folding. On the other hand, at the knot-optimal temperature of $0.35\epsilon/k_B$ the nascent conditions produce only 6.6% of the misfolded states.

Fig. 5 shows five snapshots of an example of a successful folding trajectory in our basic model of 1J85. (A related movie is available as the Supplementary Material). The sequential fragments emerge from the model ribosome in order: first green, then red, green again, and finally purple. At stage A, there is no tertiary order yet. At stage B, the knot-loop segment (75-95) has left the model ribosome. At stage C, the knot-loop forms a nearly planar and nearly closed contour and residue 121 arrives at the plane of this contour. Another perspective on this stage is shown in Fig. 6 where the knot-loop is shaded in red. The C-terminal part (121-156, in purple) of the protein must drag through the knot-loop and the success rate depends on how well residue 121 is pinned to the plane of the knot-loop. There are eight OV-based contacts that residue 121 makes with the knot-loop, as shown in Fig. 7. However, the stabilization of the attachment is enhanced by the CSU-derived contact 88-121. A fully formed slipknot is shown in panel D of Fig. 5 and, in more details, in Fig. 8. At the very next stage E, the protein gets detached from the ribosome and becomes knotted because the C-terminal segment goes through the knot-loop.

Our results confirm the picture proposed in ref. [11] that knotting in 1J85 is enabled by the slipknotting mechanism. However, we see it operational only when the protein is nascent. The wall facilitates formation of the C-terminal slipknot on the correct side of the knot-loop and it provides semi-confinement that allows for making repeated attempts to drag the slip-loop through the knot-loop. When one removes the wall but starts the evolution from the slipknot conformation, then – at optimality – 75% of trajectories lead to the knot formation.

It is interesting to note that inclusion of the 88-121 contact, at $T = 0.35\epsilon/k_B$ and for $t_w=5000 \tau$, boosts S from 3.0% to 4.8%. An inclusion of all missing CSU contacts (the OV-CSU contact map) boosts it even further to 6.2%. All of these contacts should be considered native. Wallin, *et al.* [35] have argued that non-native contacts are necessary to fold 1J85 to the knotted state. Specifically they added exponentially decaying non-native contacts between segments [86,93] and [122,147]. Their definition of a native contact is that two heavy atoms from different residues must fall within the distance of 4.5 Å from one another. This procedure misses the 88-121 contact. In our contact map, we generate 13 OV native contacts for the segments chosen by Wallin *et al.*. CSU adds 4 more and 88-121 is the fifth one. Thus there is no need to invoke non-native contacts to explain folding in 1J85.

3.4 The energetics of the slipknot formation during folding on the ribosome

We have observed that the knotting process is very rapid. It takes quite a long time for a protein to get to state (a) shown in Fig. 9, in which the slip-loop is positioned just above the knot-loop. We expect that the specific amino-acid arrangement leads to formation of a potential well and, therefore, emergence of a force that drags the slip-loop through the knot-loop. To prove this, we have monitored the potential energy associated with specific amino acids from the slip-loop. The top panels in Fig. 9 show the energy experienced by one of the amino acids from the slip-loop, the 125th in the sequence, if found at various locations within the plane parallel to the plane of the model ribosome and crossing through this amino acid. The potential well is very localized. In state (a), its

depth is close to 0.50ϵ and in state (b), 200τ later, it increases to 1.0ϵ . In state (c), the slipknot is already created and the well becomes very shallow – 0.07ϵ – and the slipknot ceases to move forward any further. If at stage (a) the conformation of the knot-loop is such that the well is not sufficiently deep then no proper knotting takes place.

3.5 Other deeply knotted proteins

We have considered two other deeply knotted (hypothetical) proteins [19]: 1O6D from *Thermatoga maritima* and 1VH0 from *Staphylococcus aureus*. Both were analyzed previously through stretching simulations [6]. We find no properly folded trajectories for 1O6D and 1VH0, either with or without the wall. However, we have obtained substantial percentages of the misfolding situations. For 1O6D, 41 out of 400 trajectories without the wall and 151 out of 400 with the wall resulted in misfolding. For 1VH0, the corresponding numbers are 136 out of 500 and 203 out of 390. Thus the ribosome-imitating wall helps in folding through semi-confinement but not sufficiently enough to form the proper knots in a noticeable way. However, more sophisticated models of the ribosome might work better.

4 Conclusions

We have used the structure-based molecular dynamics model to study folding of deeply knotted proteins. The structure-based models favor formation of the native contacts but carry no topological bias. It is an open question how to implement such a bias in a model. Establishment of the native contacts usually does not mean establishing the knot. The nascent conditions are found to enhance the probability of establishing the contacts and sometimes also the formation of the knot. We also find that achieving proper folding requires staying within the proper range of temperatures.

Our results are consistent with the experiments of Mallam *et al.* [36] that nascent proteins form knots more easily and that knots in 1J85 (YibK) persist in the chemically denatured state [37]. Independent of this, the GroEL-GroES chaperonin complex may also accelerate knotted folding [36].

Our results for 1J85 support the slipknot mechanism in the knot formation but suggest that it may operate only under the nascent conditions and when the temperature is within an optimal range. The geometry of the ribosome tunnel should provide even more confinement than that given just by the plane and should boost the efficiency of cotranslational folding. Finally, there is no need to invoke non-native contacts to fold to the knotted state in this system.

Proteins with shallow knots, such as MJ0366 from *Methanocaldococcus jannaschii* with the PDB structure code of 2EFV, studied theoretically in refs. [38, 39] appear to fold in a different way both off- and on-ribosome. A discussion of this problem is being prepared for a separate report.

Acknowledgments We appreciate useful discussions with J. Trylska. This work has been supported by the ERA-NET-IB/06/2013 Grant FiberFuel funded by the National Centre for Research and Development in Poland. The local computer resources were financed by the European Regional Development Fund under the Operational Programme Innovative Economy NanoFun POIG.02.02.00-00-025/09.

References

- [1] Virnau P, Mirny L A, Kardar M 2006 *Plos. Comp. Biol.* **2** e122
- [2] Virnau P, Mallam A, Jackson S 2011 *J. Phys. Cond. Mat.* **23** 033101
- [3] Sułkowska J I, Rawdon E J, Millet K C, Onuchic J N, Stasiak A 2012 *Proc. Natl. Acad. Sci. USA* **109** E1715-E1723

- [4] Koniaris K, Muthukumar M 1991 *Phys. Rev. Lett.* **66** 2211-2214
- [5] Taylor W 2000 *Nature* **406** 916-919
- [6] Sułkowska J I, Sułkowski P, Szymczak P, Cieplak M 2008 *Phys. Rev. Lett.* **100** 058106
- [7] Sułkowska J I, Sułkowski P, Szymczak P, Cieplak M 2010 *J. Am. Chem. Soc.* **132** 13954-13956
- [8] Dziubiella J 2009 *Biophys. J.* **96** 831-839
- [9] Chwastyk M, Cieplak M 2014 *Israel Journal of Chemistry* **54** 1241-1249
- [10] Dill K A, MacCallum J L 2012 *Science* **338** 1042-1046
- [11] Sułkowska J I, Sułkowski P, Onuchic J N 2009 *Proc. Natl. Acad. Sci. USA* **106** 3119-3124
- [12] Li W, Terakawa T, Wang W, Takada S 2012 *Proc. Natl. Acad. Sci. USA* **109** 17789-17794
- [13] Cabrita L D, Dobson C M, Christodoulou J 2010 *Curr. Op. Struct. Biol.* **20** 33-45
- [14] Kaiser C M, Goldman D H, Chodera J D, Tinoco Jr. I, Bustamante C 2011 *Science* **334** 1723-1727
- [15] Melnikov S, Ben-Shem A, Garreau de Loubresse N, Jenner L, Yusupova G, Yusupov M 2012 *Nat. Struct. Mol. Biol.* **19** 560-567
- [16] Garreau de Loubresse N, Prokhorova I, Holtkamp W, Rodnina M V, Yusupova G, Yusupov M 2014 *Nature* **513** 517-522
- [17] Voss N R, Gerstein M, Steitz T A, Moore P B 2006 *J. Mol. Biol.* **360** 893-906
- [18] Frank J, Gonzales R L Jr. 2010 *Annu. Rev. Biochem.* **79** 381-412
- [19] Badger J, Sauder J M, Adams J M *et al.* 2005 *Proteins* **60** 787-796
- [20] Lim K, Zhang H, Tempczyk A, Krajewski W, Bonander N, Toedt J, Howard A, Eisenstein E, Herzberg O 2003 *Proteins* **51** 56-67
- [21] Go N 1983 *Annu. Rev. Biophys. Bioeng.* **12** 183-210
- [22] Sułkowska J I and Cieplak M 2007 *J. Phys.: Cond. Mat.* **19** 283201
- [23] Sułkowska J I, Cieplak M 2008 *Biophys. J.* **95** 3174-3191
- [24] Sikora M, Sułkowska J I, Cieplak M 2009 *PLOS Comp. Biol.* **5** e1000547
- [25] Tsai J, Taylor R, Chothia C, Gerstein M 1999 *J. Mol. Biol.* **290** 253-266
- [26] Sobolev V, Sorokine A, Prilusky J, Abola E E, Edelman M 1999 *Bioinformatics* **15** 327-332
- [27] Elcock A H 2006 *PLOS Comp. Biol.* **2** e98
- [28] Sikora M, Sułkowska J I, Witkowski B S, Cieplak M 2010 *Nucl. Acids Res.* **39** D443-D450
- [29] Socci N D, Onuchic J N 1994 *J. Chem. Phys.* **101** 1519-1528
- [30] Cieplak M and Banavar J R 2013 *Phys. Rev. E. Rapid Comm.* **88**, 040702(R)
- [31] Cieplak M and Banavar J R 2013 *EPL* **104** 58001
- [32] Cieplak M, Hoang T X 2003 *Biophys. J.* **84** 475-488
- [33] Cieplak M, Sułkowska J I 2005 *J. Chem. Phys.* **123** 194908
- [34] Clementi C, Nymeyer H, Onuchic J N 2000 *J. Mol. Biol.* **298** 937-953
- [35] Wallin S, Zeldovich K B, Shakhnovich E I 2007 *J. Mol. Biol.* **368** 884-893

- [36] Mallam A L, Jackson S E 2012 *Nat. Chem. Biol.* **8** 147-153
- [37] Mallam A L, Rogers J M, Jackson S E 2010 *Proc. Natl. Acad. Sci. USA* **107** 8189-8194
- [38] Beccara S A, Skrbic T, Covino R, Micheletti C, Faccioli P 2013 *PLOS Comp. Biol.* **9** e1003002
- [39] Noel J K, Onuchic J N, Sułkowska J I 2013 *Phys. Chem. Lett.* **4** 3570-3573

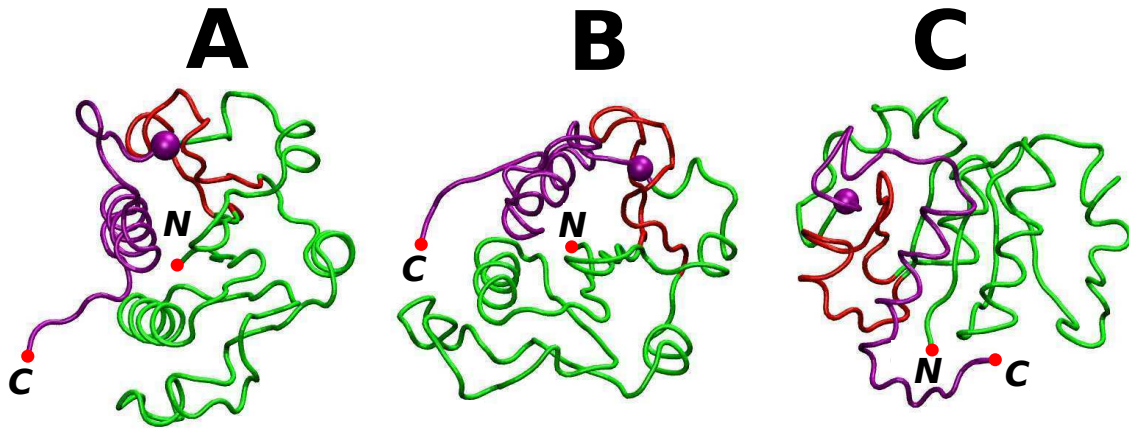


Figure 1: Panel A shows the native structure of protein 1J85. Panel B shows an example of the correctly folded state obtained through cotranslational evolution. Panel C shows an example of conformation with the native contacts all established but without the topology of the knot. The meanings of the colors are explained in the main text.

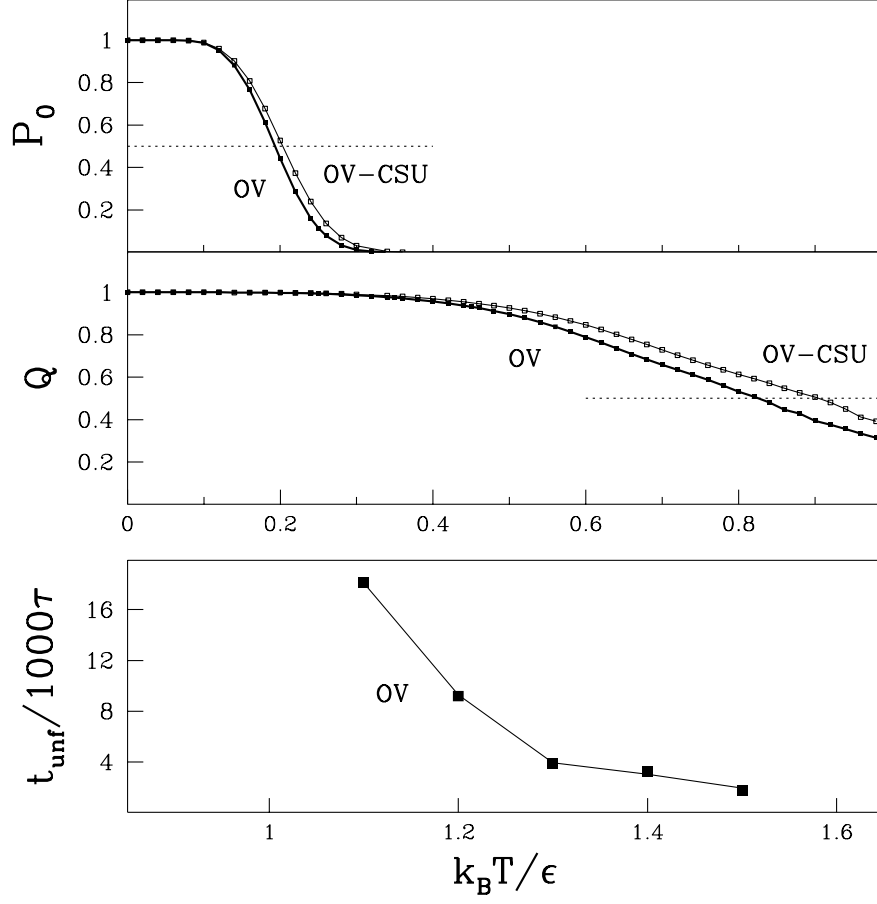


Figure 2: The temperature-dependence of P_0 , Q , and t_{unf} for 1J85, top to bottom panels correspondingly. The contact map used is indicated. The horizontal dotted lines in the top two panels correspond to the value of $\frac{1}{2}$.

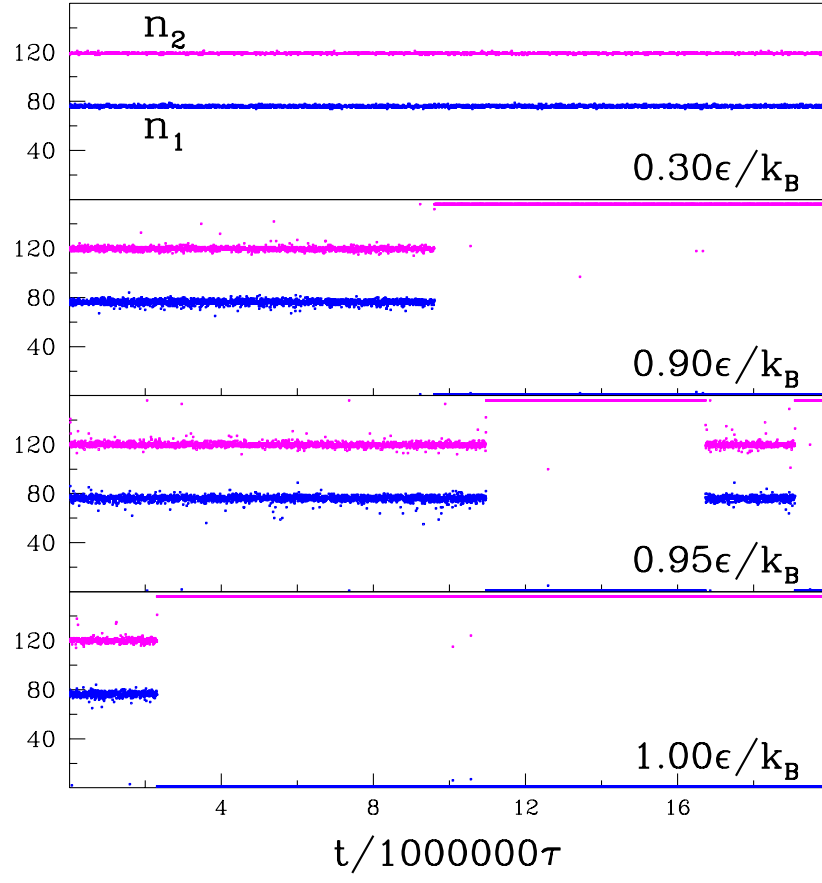


Figure 3: Locations of the knot ends in 1J85 at various temperatures as indicated.

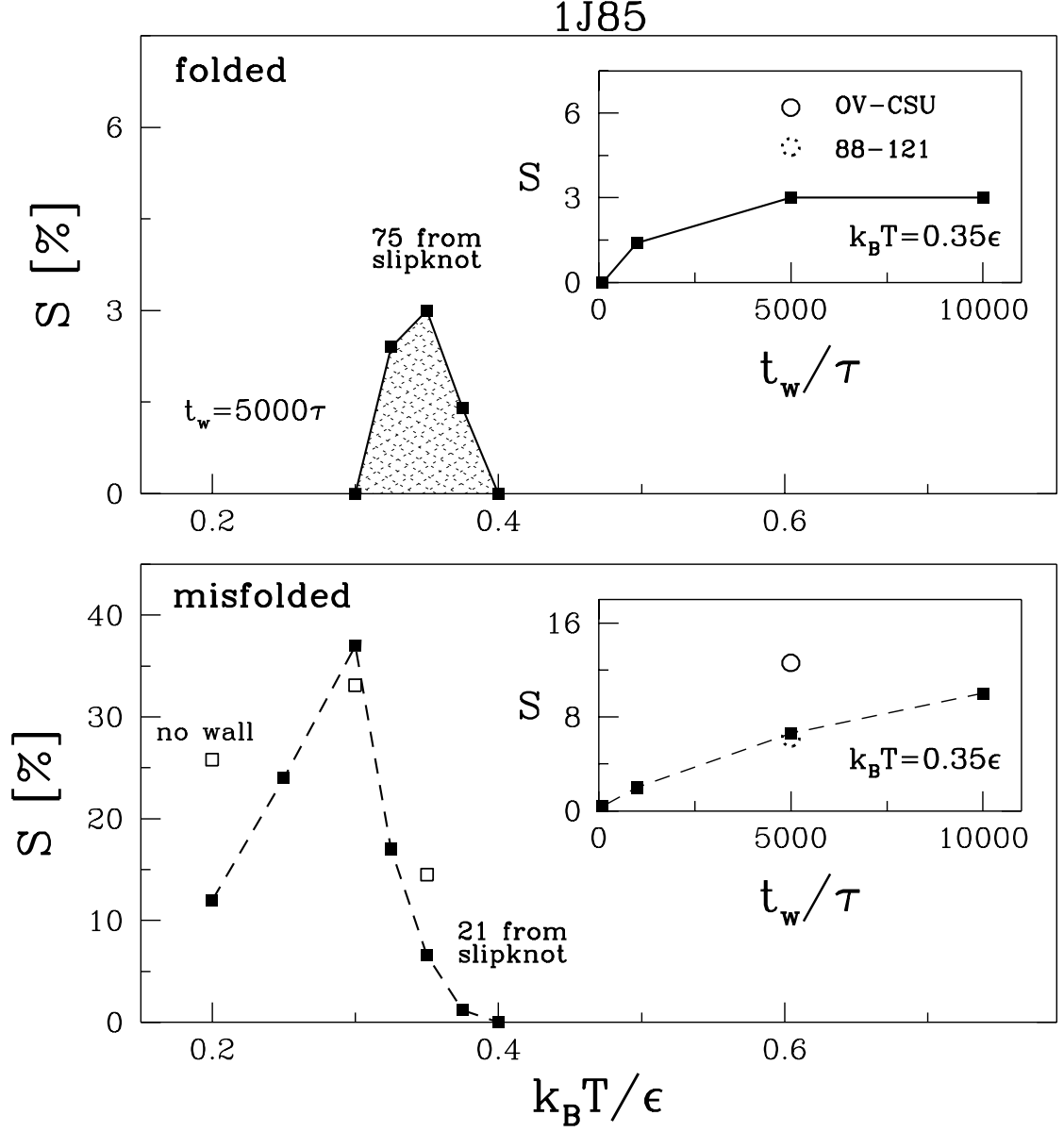


Figure 4: 1J85: the kinetic results for the on-ribosome folding. The upper panel shows the percentage-wise success in folding as a function of T for $t_w=5000 \tau$. The inset shows S as a function of t_w for the optimal temperature of $0.35 \epsilon/k_B$. The dotted circle shows S when one contact, 88-121 is added. The full circle shows S when all specific CSU contacts are added. The lower panel with its inset is similar but shows the data for misfolding – when the native contacts get established but the knot is not formed.

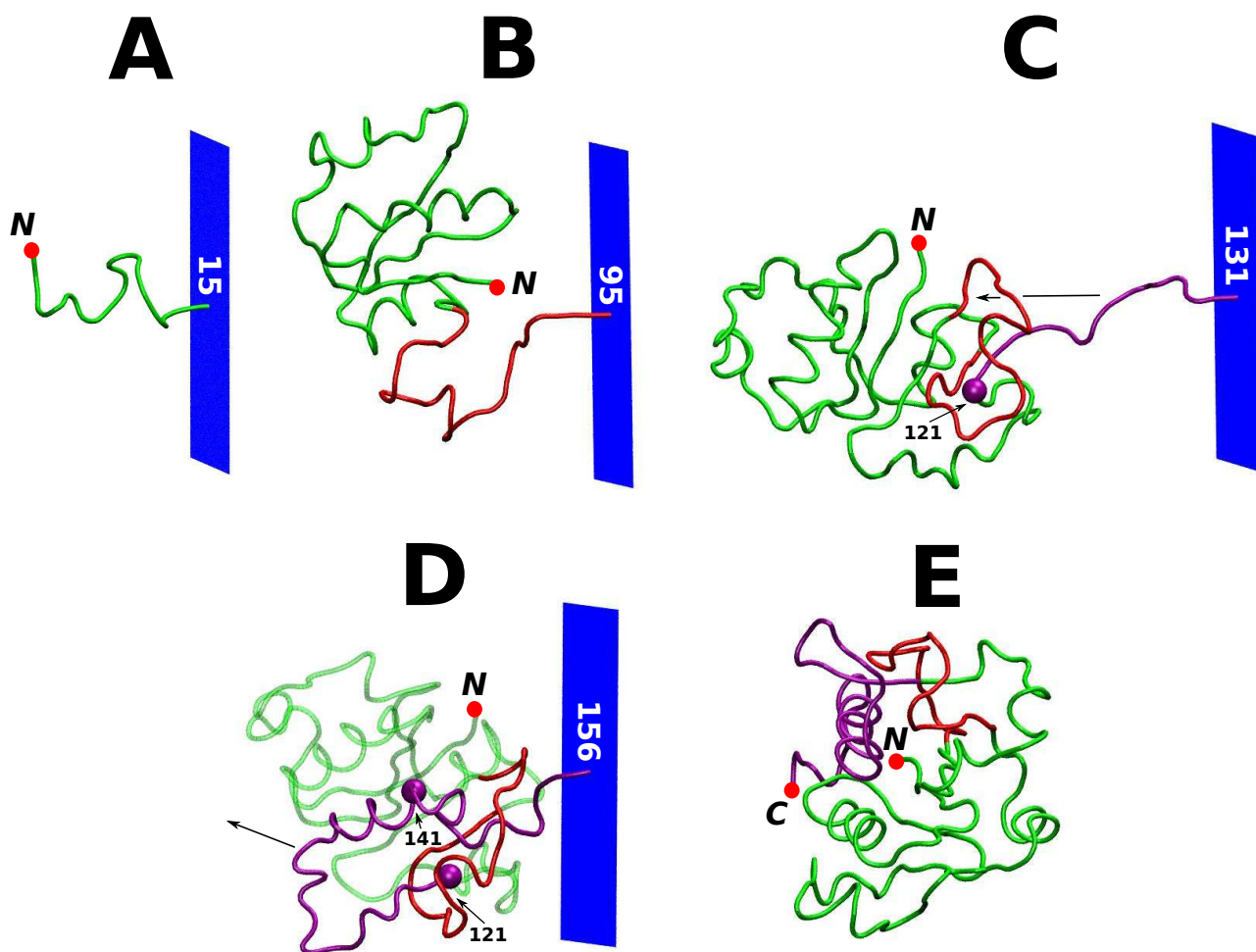


Figure 5: Stages of folding and knotting process of protein 1J85 in the presence of the repulsive wall. The wall is represented by the blue plate. The number written on the plate indicates the residue that has just been born. The part of the protein which creates the loop is marked in red color. Residue 121 is represented by a purple ball in panel C – it is the beginning of a slipknot part. The arrows in panels C and D indicate the direction in which the remaining part of the backbone moves through the red loop. The completely knotted, folded and released protein is presented in panel E without the wall as the protein gets detached.

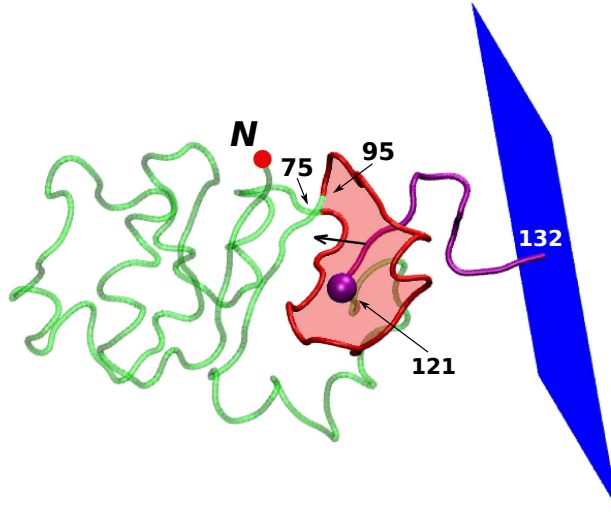


Figure 6: Conformation of the nascent 1J85 just before formation of the slipknot state. Residue 121, represented by a purple ball, stays pinned to the shaded surface spanned by the red knot-loop. In order to form the knot, the remaining C-terminal part of the protein has to drag through the knot-loop in the direction shown by the arrow.

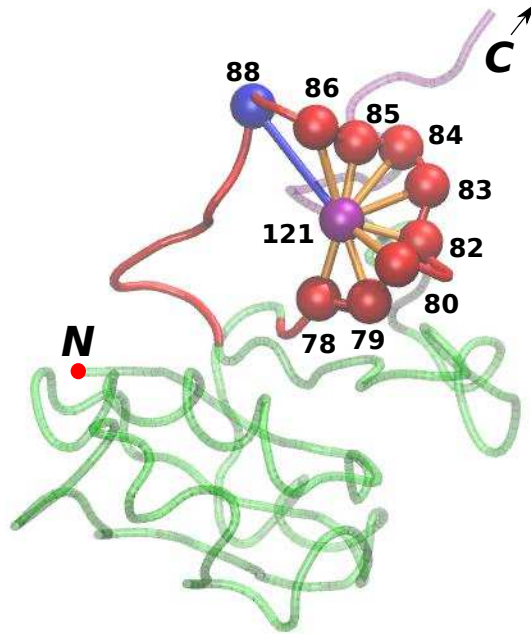


Figure 7: The contacts involving residue 121 in 1J85. The contacts shown in the orange color are derived through the overlap criterion. The contact shown in the blue color is an extra contact derived through the CSU approach. All of these contacts are with the residues that are a part of the red knot-loop.

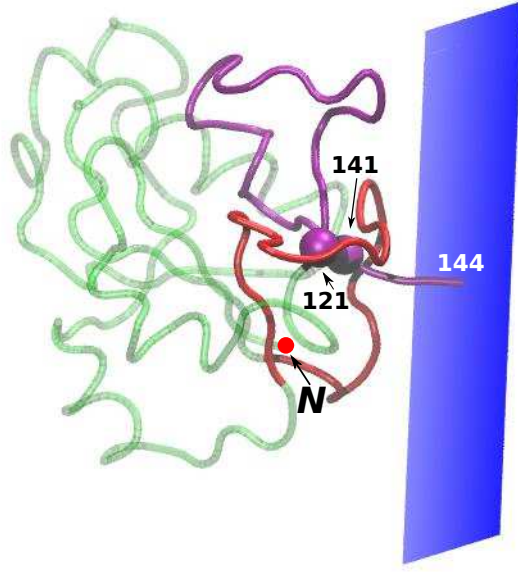


Figure 8: The fully formed slipknot state in 1J85: the purple part of the backbone just went through the red knot-loop. The purple spheres indicate the beginning (121) and ending (141) residues in the slip-loop.

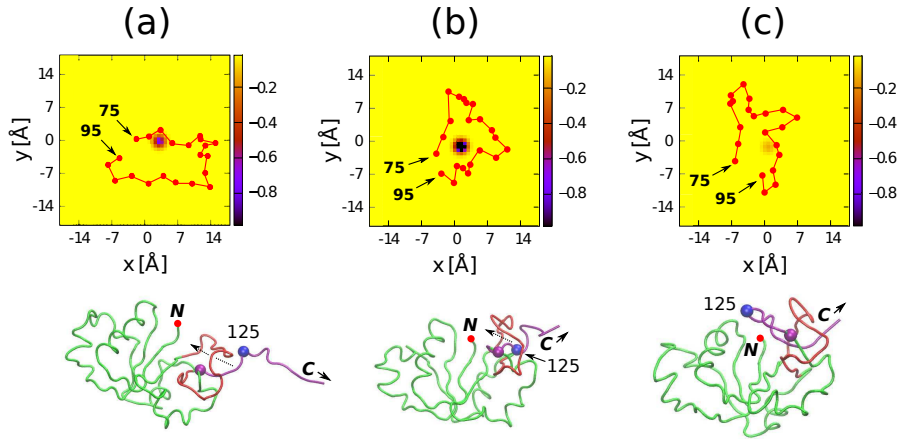


Figure 9: Three successive stages of the successful knotting process of protein 1J85 in the presence of the repulsive wall. The upper panels show the potential energies associated with amino acid 125 in units of ϵ , as indicated by the color scales on the right. The chain shows the projection of the knot-loop onto the $x - y$ plane which is parallel to the repulsive plane. The origin (0,0) is set at location of amino acid 125. The lower panels show the corresponding conformations of the protein. The thick arrow next to C indicate the sequential direction toward the C terminus which is not yet born. The dotted arrows indicate the direction of movement of amino acid 125. Panel (a) is for the situation in which the slipknot is about to be formed and panel (c) just after it was fully formed.